Growth dynamics of L-cysteine SAMs on single-crystal gold surfaces: a metastable deexcitation spectroscopy study

2009 J. Phys.: Condens. Matter 21 264005

(http://iopscience.iop.org/0953-8984/21/26/264005)

J. Phys.: Condens. Matter **21** (2009) 264005 (7pp) doi:10.1088/0953-8984/21/26/264005

Growth dynamics of L-cysteine SAMs on single-crystal gold surfaces: a metastable deexcitation spectroscopy study

M Canepa[1,4], L Lavagnino[1], L Pasquali[2], R Moroni[1], F Bisio[1], V De Renzi[3], S Terreni[1] and L Mattera[1]

[1] CNISM and Department of Physics, University of Genova, via Dodecaneso 33, I-16145 Genova, Italy
[2] Department of Materials Engineering, University of Modena and Reggio Emilia, Italy
[3] Department of Physics, University of Modena and Reggio Emilia, Italy

E-mail: Canepa@fisica.unige.it

Received 28 October 2008
Published 11 June 2009
Online at stacks.iop.org/JPhysCM/21/264005

Abstract

We report on a metastable deexcitation spectroscopy investigation of the growth of L-cysteine layers deposited under UHV conditions on well-defined Au(110)-(1 × 2) and Au(111) surfaces. The interaction of He^* with molecular orbitals gave rise to well-defined UPS-like Penning spectra which provided information on the SAM assembly dynamics and adsorption configurations. Penning spectra have been interpreted through comparison with molecular orbital DFT calculations of the free molecule and have been compared with XPS results of previous works. Regarding adsorption of first-layer molecules at room temperature (RT), two different growth regimes were observed. On Au(110), the absence of spectral features related to orbitals associated with SH groups indicated the formation of a compact SAM of thiolate molecules. On Au(111), the data demonstrated the simultaneous presence, since the early stages of growth, of strongly and weakly bound molecules, the latter showing intact SH groups. The different growth mode was tentatively assigned to the added rows of the reconstructed Au(110) surface which behave as extended defects effectively promoting the formation of the S–Au bond. The growth of the second molecular layer was instead observed to proceed similarly for both substrates. Second-layer molecules preferably adopt an adsorption configuration in which the SH group protrudes into the vacuum side.

(Some figures in this article are in colour only in the electronic version)

1. Introduction

Cysteine [Cys, HS–CH_2–CH(NH_2)–COOH] is a fundamental amino acid which plays an important role as a linker of biomolecules with metal surfaces [1–5]. The Cys/gold interaction is important in the field of biosensors [6–8]. Seminal studies on the Cys/gold system date back to the early 1990s [9, 10]. Recently, cysteine adsorption on gold has been exploited in studies of enantioselectivity processes at the surface of single crystals [11, 12] and clusters [13]. Cysteine has also been found to induce chiral electronic states in an initially achiral polycrystalline Au film [14]. Cysteine also provided an interesting method for tailoring optical properties of gold nanoparticles, by promoting transverse overgrowth of nanorods [15]. Further, the interaction of cysteine with gold colloids has also been exploited in heterogeneous catalysis studies [16]. The chameleonic ability of amino acids to form molecular networks is known to lead to very complex phase diagrams at surfaces [17]. When deposited from the liquid phase, the structural properties of cysteine self-assembled monolayers (SAMs) subtly depend on the pH and on the electrochemical potential conditions, which affect the charge state of the molecule [18–22]. A rich variety of interesting nanostructures also develops under ultra-high vacuum (UHV) evaporation conditions [23–25] and Cys SAMs have been

[4] Author to whom any correspondence should be addressed.

proposed as case studies to investigate hydrogen bonds in 2D networks [26].

Concerning the Cys–Au bond, a large amount of information has been derived by x-ray electron spectroscopy [10, 26–29], exploiting the comparison with the wide database available on thiolate SAMs. Application of valence-state spectroscopies, which would allow for a more direct comparison with calculations of bonding properties [30], is instead rare [29].

In this paper we report on the application of metastable deexcitation spectroscopy (MDS), i.e. the spectroscopy of electrons ejected after metastable helium (He^*) deexcitation at surfaces (elsewhere denoted as MAES or MIES), to the study of L-cysteine layers deposited under UHV conditions on well-defined gold surfaces. MDS has been known for many years as a valuable tool to study the valence band structure of adsorbate-covered surfaces [31–35]. In particular, the enhanced sensitivity to molecular adsorbates through the Penning ionization (PI) process prompted a systematic application of MDS to organic SAMs [36–41]. Though the metastable atom beam is known to cause some damage effects in soft matter layers [42], since atomic deexcitation occurs in the vacuum region just outside the surface, MDS turns out to be less perturbative than photon-in spectroscopies which produce a huge number of electrons in the first few layers of the solid. In this work we obtained a reliable set of data on the valence states of adsorbed Cys. Comparison with DFT calculations was exploited to interpret the data, allowing us to discriminate strongly and weakly bound molecules and to shine light on the different growth dynamics on Au(110) and Au(111), as a function of coverage and deposition temperature, which was still under question [23–26].

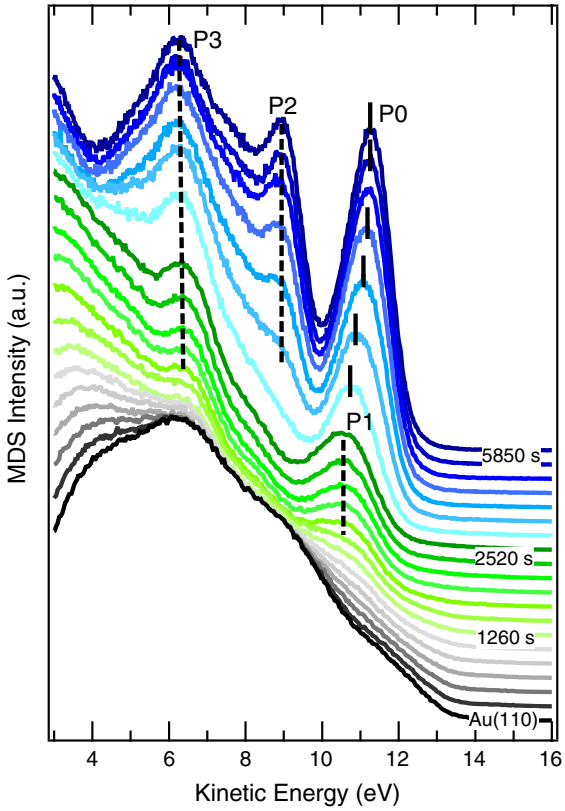

Figure 1. MDS electron energy distribution curves (EDCs) measured as a function of exposure time during L-cysteine deposition on the Au(110)-(1 × 2) surface at room temperature. Attenuation of features related to the He^* Auger neutralization process on clean surface patches is followed by the transition to the Penning ionization at cysteine orbitals.

2. Experimental details

Details on the experimental apparatus can be found elsewhere [43]. Here only summary information is provided. The He^* beam is produced in a dc discharge. The intensity of the 2^3S fraction on the sample is of the order of 10^{11} at. s^{-1} with negligible percentages of 2^1S atoms and UV photons. The apparatus geometry allows MDS real-time monitoring of film deposition. Clean, well-ordered metal surfaces were prepared by sputtering and annealing cycles, according to well-known procedures [24, 28, 26]. L-cysteine powders (purity 99%, Sigma) were used after re-crystallization in Milli-Q water. Deposition was performed by a differentially pumped molecular beam source fully described in [43] and already used in several experiments [24, 28, 26]. An operating temperature of about 100 °C was chosen to avoid cysteine cracking. The pressure rise in the analysis chamber during deposition amounted to a few units in the 10^{-10} mbar scale. The damage effects produced by the He^* beam on Cys SAMS were considered in [43].

3. Experimental results

Figure 1 shows the evolution of electron energy distribution curves (EDCs) measured during slow deposition on the Au(110)-(1 × 2) surface at room temperature. The smooth shape of the clean surface EDC resulted from the Auger neutralization of the ion after the resonant ionization of the incoming He^* atom [32, 44, 45]. The two-electron AN spectra from metal surfaces are often rationalized as the self-convolution of an effective surface density of states [31, 46]. At early stages of deposition, following the general attenuation of the AN features, relatively broad adsorbate-induced features developed into UPS-like Penning peaks at about 10.6–10.7 eV KE (P1) and 6.3 eV KE (P3). Continuing with Cys exposure, the parallel growth of a pair of intense and relatively narrow peaks, P0 and P2, was observed. P0 grew at the highest energy side of P1. Its position at saturation was 11.3 eV KE. P2 emerged from a monotonic background at about 9 eV KE. The peak P3 evolved into a relatively intense structure with evident side shoulders. Below 4 eV KE, the presence of Penning peaks was completely obscured by the background of secondaries. Saturation of spectra was observed for roughly twice the Cys dose necessary to saturate P1.

Measurements on Au(111) at RT are shown in figure 2. Several elements were at variance with the Au(110) case. The most evident difference regarded the shape of the first Penning features which developed from the AN background. In comparison to the P1 peak of figure 1, one observed here a broader feature roughly centred at about 11 eV and

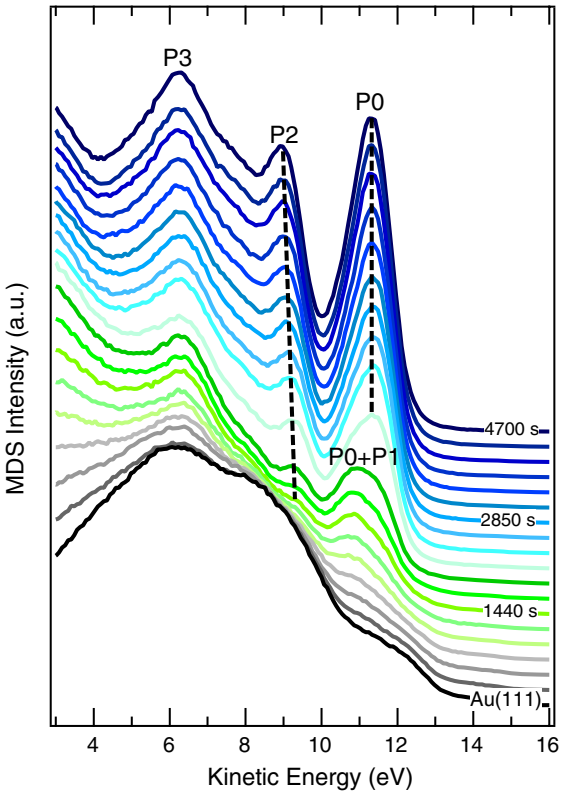

Figure 2. MDS electron energy distribution curves (EDCs) measured during L-cysteine deposition on the Au(111) surface at room temperature.

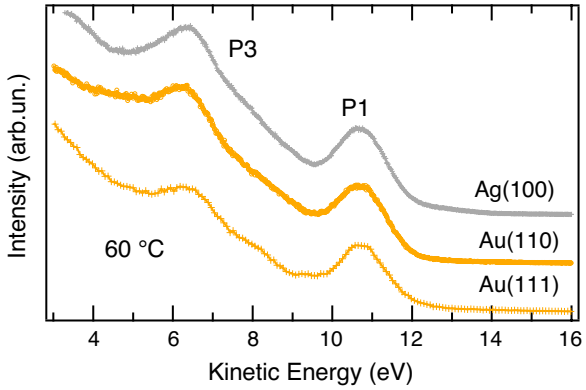

Figure 3. MDS electron energy distribution curves (EDCs) measured at saturation for L-cysteine deposition on the Au(111), Au(110) and Ag(001) surfaces at 60 °C.

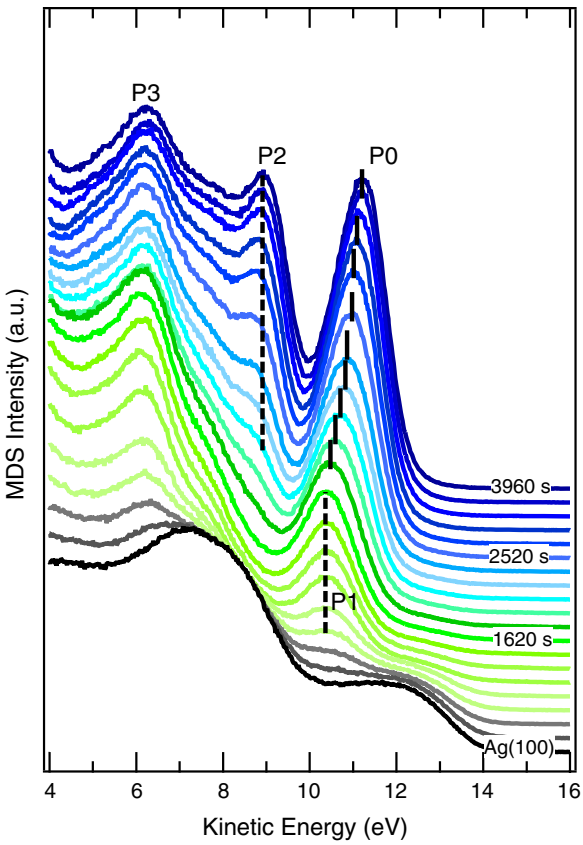

Figure 4. MDS electron energy distribution curves (EDCs) measured during L-cysteine deposition on the Ag(100) surface at room temperature. The KE position of Penning peaks is the same, within experimental uncertainty, as in figure 1.

accompanied by a small peak at about 9.2 eV KE. The asymmetric shape of the highest KE feature suggested the superposition of two sub-components at about 10.6 eV KE and 11.2–11.4 eV. These initial features had an influence also on the subsequent spectral evolution of the P0–P2 pair. P0 was found in fact to grow at practically constant energy while P2 slightly shifted left, to about 9 eV. Remarkably, the fully saturated spectra looked absolutely similar, regarding intensity, peak lineshape and position, to those of figure 1.

For both substrates, the P0–P2 features were unstable for temperatures slightly higher than RT. In figure 3, we report the saturation spectra obtained for a 60 °C deposition temperature. Closely similar results were found on both Au(110) and Au(111). Only two peaks were visible, at about 10.6 and 6.3–6.4 eV. The same results were also obtained after annealing at 60 °C RT-deposited saturated phases (i.e. after full evolution of the P0–P2 pair). The P1–P3 features were instead definitely more stable against both thermal treatments and beam erosive action [43]. Major changes occurred only above 130–140 °C where, consistent with thermal programmed desorption data [47], a transition to the RI+AN deexcitation path, indicative of molecular desorption, was observed.

The growth dynamics found on Au(110) (growth and apparent saturation of P1 followed by growth of the P0–P2 pair) was observed also on the Cu(100) surface [43] and in the case of Ag(100). The MDS measurements on Ag(100) are shown in figure 4 (RT deposition) and figure 3 (deposition at 60 °C). In figure 4 the characteristic 'staircase' shape of the silver AN spectra [46] made the evolution of Cys-related Penning peaks particularly clear. The KE position of Penning peaks is the same, within experimental uncertainty, as in figure 1.

4. Discussion

Adsorption states of thiolate species are usually identified through the analysis of XPS S2p core level shifts [48, 49].

Table 1. UHV deposition of cysteine on gold surfaces. Summary of MDS data and literature XPS data. (Note: $S_{th} \sim 162$ eV BE $S_{un} \sim 164.2$ eV BE; P1 ≈ 10.6 eV KE P2 ≈ 9 eV KE.)

Surface	Deposition temperature	XPS peaks	Reference	High KE MDS peaks
Au(110) [a]	RT	S_{th}	[28]	P1
Au(111) [a]	RT	S_{th}, S_{un}	[26]	P1, P0–P2
Au(110) [b]	RT	S_{th}, S_{un}	[28]	P0–P2
Au(111) [b]	RT	S_{th}, S_{un}	[26]	P0–P2
Au(110)	60 °C	S_{th}	[28, 24]	P1
Au(111)	60 °C	S_{th}	[26]	P1

[a] Low coverage.
[b] High coverage.

Therefore, it seems useful to present a concise review of available XPS data for the Cys/gold system to be compared with MDS observations. On Au(110), at RT, a state at about 162 eV BE was observed at submonolayer coverage and assigned to the S–Au bond (S_{th} for brevity) [28]. Increasing the coverage after saturation of the S_{th} state, a second state, S_{un}, was observed at 164.2 eV BE. S_{un} vanished after annealing at moderate temperatures (60 °C) and was assigned to the unreacted SH group of second-layer molecules [28]. S_{th} also vanished above 130 °C, while a third component appeared at about 161 eV, accompanied by a severe loss of intensity of the N 1s, C 1s and O 1s peaks, indicating a deep alteration of the molecular layer [28]. On Au(111), at RT, XPS measurements indicated, even at relatively low coverage, the coexistence of S_{th} and S_{un} states [26]. The S_{th} component alone was detected only in the limit of very low coverage. Similarly to the case of Au(110), annealing of a high coverage phase at 60 °C or direct deposition at 60 °C led to the S_{th} component only [26]. We note that for adsorption from solution on gold films presenting a (111) texturing, only the S_{th} component was detected [27, 29]. A summary of the MDS/XPS results is reported in table 1.

In order to help the interpretation of MDS spectra we performed DFT calculations of the electronic structure of the free neutral molecule. Calculations for Cys adsorption on Au(111) available in the literature were also considered [30, 50]. In our calculations, the equilibrium geometry and the valence orbital properties of the free molecule were calculated using the StoBe code [51] and applying a gradient-corrected RPBE exchange/correlation functional [52, 53]. All-electron triple-ζ valence plus polarization (TZVP) atomic Gaussian basis sets for S, C, O and N centres were adopted. A (311/1)-type hydrogen basis set was chosen [54]. Different molecular configurations were tested and attention was focused on the geometry represented in figure 5. The figure shows isosurface plots of selected orbitals. Total and projected density of states (DOS) on the different molecular groups were superimposed, after a 0.7 eV Gaussian broadening, on MDS spectra taken at saturation, having aligned the calculated HOMO (orbital 32) to the P0 peak. The kinetic to binding energy scale conversion was obtained by comparison with UPS results obtained at the BEAR beamline (ELETTRA, Trieste) and data in the literature [29]. First, the MDS/UPS KE spectra have been aligned by shifting the MDS pattern of the amount $h\nu - E_{exc}$, $h\nu$ being the UPS photon energy (60 eV) and E_{exc} the MDS excitation energy (19.8 eV). Then, the spectra have been transposed into the binding energy scale referenced to the UPS Fermi edge. We observed a good alignment of the MDS P3 peak with a corresponding structure of the UPS spectra at about 9 eV BE, out of the gold d bands [29]. After the prominent HOMO peak, the calculations show a peak (orbitals 30 and 29), mainly localized on the COOH and NH_2 groups, at about 5 eV, where the data presented a rather deep minimum. The position of orbital 28, strongly localized on the SH group, nicely agree with the experimental P2 peak. Moving to the low KE side, the increasing number of overlapping orbitals to be considered and the influence of the background of secondary electrons, made the comparison between data and calculations more and more difficult. It is worth noting that orbitals which give rise to the P3 structure are expected to be poorly affected by the molecule–metal bond. We therefore focused attention on the highest KE peaks and in particular on the HOMO energy region.

The assembly of the first layer (about 0.5 nm thick [55]), which progressively 'shielded' the substrate from the incoming He^*, explains the regular decay of the Auger neutralization emission from the metal observed in the early deposition stages. On Au(110) (figure 1) the suppression of the AN features is accompanied by the growth of P1 at constant energy. At this stage of deposition, the absence of the P0–P2 pair is consistent with the S–Au reaction and with the formation of the compact SAM which led to the full removal of the 1×2 reconstruction of the clean substrate [23, 24]. We will address the assignment of P1, which was also found for adsorption at 60 °C (figure 3) later in this discussion. The growing P0–P2 pair, progressively masking the P1 feature, is to be assigned to second-layer molecules, with an 'unreacted' SH group, which eventually detached from the surface after a mild annealing. Such interpretation is fully consistent with XPS assignments of previous works (cf table 1).

On Au(111), the shape of the Penning spectrum which emerged from the decaying AN background (figure 2) neatly differed, especially in the highest KE range, from the Au(110) case, confirming a different growth dynamics of the first layer. A key feature is the asymmetric shape of the broad feature at about 11 eV KE, indicated as P0+P1 in figure 2. As suggested by the labelling, a possible interpretation assigns the P0 sub-component (at about 11.3 eV KE) and the P2 peak to molecules with unreacted SH groups. The left-hand side component of the P1+P0 feature, appreciable in figure 2 at about 10.6 eV KE, could then be assigned to an Au(110)-like P1 state of strongly adsorbed molecules. The hypothesis of a superposition of states belonging to strongly bound (via the S–Au bond) and weakly bound molecules would be fully consistent with XPS results (cf table 1) and with STM findings [25]. However, looking at simulations of figure 4, a contribution to the intensity of the left-hand side of the P1 + P0 peak from orbitals 29 and 30 of weakly adsorbed molecules should be considered as well.

Indeed, the Cys/Au(111) system was theoretically examined under a DFT approach a few years ago [30, 50]. A number of different adsorption configurations were tested

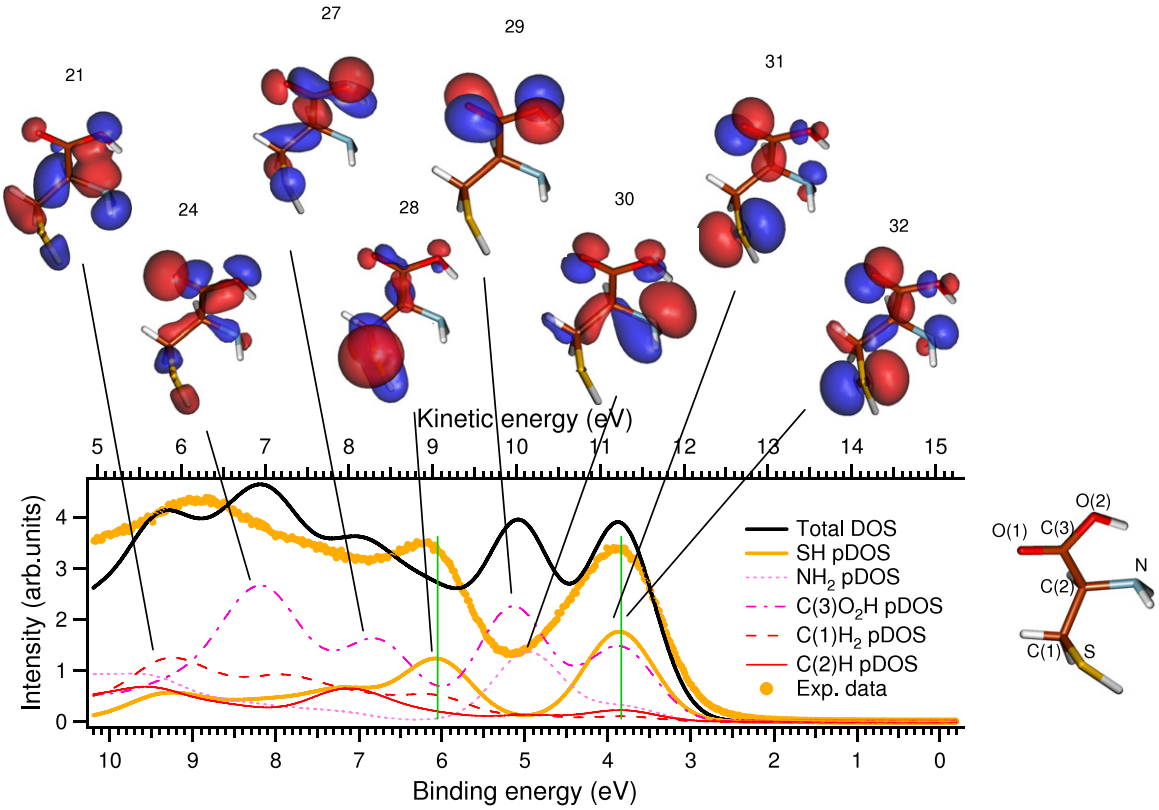

Figure 5. Free-molecule DFT calculations of the total and projected DOS on the different molecular groups. Calculations were performed using the StoBe code [51] for the molecular configuration represented in the right part of the figure. Calculations, shown after a 0.7 eV Gaussian broadening, are compared with MDS data at saturation on Au(111), without background subtraction. The calculated HOMO (orbital 32) has been aligned to the MDS P0 peak. The kinetic to binding energy scale conversion was obtained by comparison with UPS results (not shown).

and total and projected density of states were calculated. A chemisorption state involving bonding through both thiol and amino groups turned out to be energetically favoured. These calculations seem not to fit our experimental findings at RT whereas they could in principle be more suitable to the data obtained for deposition at 60 °C. The position of the MDS P1 state of figure 3 would be consistent with an assignment to a Cys–Au bonding state, calculated in the 4.5–6 eV binding energy range [50]. However, two aspects induce caution about such an interpretation and encourage the search for an alternative interpretation of the P1 peak. First, the lack of observation of any spectral features which could be related to antibonding states, expected closer to the Fermi energy in the 0–2 eV binding energy range [50]. Second, the fact that similar patterns were observed on metals, such as Au and Ag (figure 4), with a very different d-band threshold energy. Taking into consideration matrix element effects, one has to consider that the Penning deexcitation process intrinsically selects those molecular orbitals whose electron density protrudes more into the vacuum side. For compact monolayers, it is conceivable that both bonding and antibonding states, whose electron density is localized at the very interface [50], are effectively shielded by outer molecular orbitals, less likely affected by the molecule–surface bond. One example of such orbitals is most probably given by the P3 state, whose position was largely independent of the type of substrate and deposition temperature. Regarding P1, we can speculate about a contribution from those molecular orbitals of zwitterionic molecules which are expected to play a major role in the building up of the molecular network. In this respect, we tentatively assign P1 to orbitals 29 and 30, most likely modified by molecular interactions. From this point of view, MDS results leave the question of a clear detection of valence interface states practically open.

Relatively strong bonds between molecules represent a clear element of difference with respect to other thiolate SAMs, e.g. alkanethiols. The different growth dynamics of Cys SAMs on Au(110) and Au(111) are indicative of some subtle interplay between the assembly properties of molecular networks and the formation of the S–Au bond. The substrate symmetry and defects are expected to play a role in such interplay. The different growth mode might be due to the added rows of the reconstructed Au(110) surface which behave as extended defects effectively promoting the formation of the S–Au bond. New energetics calculations, which consider explicitly the molecular interactions and take into account the possible zwitterionic character of the molecules, are necessary to get an insight into this interesting aspect.

A final intriguing point regards second-layer molecules. For these weakly bound molecules the comparison with free-molecule calculations can be made more stringent. The comparison between data and calculations and the spectral

evolution suggest a preferential interaction of the He^* atom with orbitals 32–31 and 28. Then, second-layer molecules, likely weakly bound to the first layer through hydrogen bonds involving NH_3^+ and COO^- groups [10], should be preferably oriented with the SH group protruding into the vacuum side. Under the exploited UHV conditions we did not observe any clear evidence of third-layer molecule adsorption. We did obtain the same saturated spectrum after massive doses of Cys, even blanking the He^* beam, or increasing the deposition rate by an order of magnitude. In this respect, it is interesting to note that MDS spectra at saturation turned out to be substantially insensitive to huge RT exposure to H_2O molecules as well.

5. Conclusions

We have presented an He^*-MDS study of L-cysteine layers deposited by molecular beam deposition under UHV conditions on Au(110) and Au(111). The observation of well-defined UPS-like Penning spectra provided information on the SAM assembly and adsorption configurations. Penning peaks have been interpreted through comparison with molecular orbital DFT (STOBE) calculations of the free molecule. Data have also been compared with XPS results of previous works. Regarding adsorption of first-layer molecules at RT, two different growth regimes were observed. On Au(110), the lack of signal from orbitals related to the SH group has been interpreted in terms of the formation of a compact SAM of thiolate molecules. On Au(111), the data demonstrated the simultaneous presence, since the early stages of growth, of strongly and weakly bound molecules, the latter showing unreacted SH groups. The different growth mode has been tentatively associated to the role of added rows of the reconstructed Au(110) surface which behave as extended defects effectively promoting the formation of the S–Au bond. The growth of the second molecular layer at RT was instead observed to proceed similarly for both substrates. For second-layer molecules, He^* was found to interact preferentially with orbitals related to the SH groups, indicating that the SH group tends to protrude into the vacuum side. At RT, under the exploited deposition conditions, we did not find any clear evidence for third-layer molecule adsorption, and the Cys bilayer was practically insensitive to water exposure. A mild substrate temperature (60 °C) was enough to inhibit second-layer growth as well. At such temperatures, the spectral features obtained on Au(111) became definitely similar to those obtained on Au(110) and on other substrates, such as Ag(100), and indicated a compact SAM of thiolate molecules.

Acknowledgments

FB and RM acknowledge an agreement between CNR and CNISM for financial support. MC warmly thanks Ornella Cavalleri and Ranieri Rolandi for drawing his attention to cysteine and Mirko Prato for helpful assistance in some stages of the work. MC thanks the staff of the BEAR beamline (ELETTRA) and in particular Dr Nicola Mahne for helpful assistance during a measurement session. This research has been supported by the University of Genova and MIUR (PRIN 2006020543003).

References

[1] Leggett G J, Roberta C J, Williams P M, Davies M C, Jackson D E and Tendler S J B 1993 *Langmuir* **9** 2356
[2] Girisha A, Sunb H, Yeoa D S Y, Chena G Y J, Chuaa T and Yaoa S Q 2005 *Bioorg. Med. Chem. Lett.* **15** 2447
[3] Uvdal K and Vikinge T P 2001 *Langmuir* **17** 2008
[4] Hansen A G, Boisen A, Nielsen J U, Wackerbarth H, Chorkendorff I, Andersen J E T, Jingdong Z and Ulstrup J 2003 *Langmuir* **19** 3419
[5] Smith E A, Wanat M J, Cheng Y, Barreira S V P, Frutos A G and Corn R M 2001 *Langmuir* **17** 2502
[6] Gooding J J, Hibbert D B and Yang W 2001 *Sensors* **1** 75
[7] Lee J-S, Ulmann P A, Han M S and Mirkin C A 2008 *Nano Lett.* **8** 529
[8] Lee S B and Martin C R 2001 *Anal. Chem.* **73** 768
[9] Ihs A and Liedberg B 1991 *J. Colloid Interface Sci.* **144** 282
[10] Uvdal K, Bodö P and Liedberg B 1992 *J. Colloid Interface Sci.* **149** 162
[11] Kühnle A, Linderoth T R, Hammer B and Besenbacher F 2002 *Nature* **415** 891
[12] Greber T, Sljivancanin Z, Schillinger R, Wider J and Hammer B 2006 *Phys. Rev. Lett.* **96** 056103
[13] Lopez-Lozano X, Perez L A and Garzon I L 2006 *Phys. Rev. Lett.* **97** 233401
[14] Bovet N, McMillan N, Gadegaard N and Kadodwala M 2007 *J. Phys. Chem.* B **111** 10005
[15] Kou X, Zhang S, Yang Z, Tsung C-K, Stucky G D, Sun L, Wang J and Yan C 2007 *J. Am. Chem. Soc.* **129** 6402
[16] Comotti M, Della Pina C, Matarrese R and Rossi M 2004 *Angew. Chem. Int. Edn* **43** 5812
[17] Barlow S M and Raval R 2003 *Surf. Sci. Rep.* **50** 201
[18] Dakkouri A S, Kolb D M, Edelstein-Shima R and Mandler D 1996 *Langmuir* **12** 2849
[19] Dodero G, De Michieli L, Cavalleri O, Rolandi R, Oliveri L, Daccá A and Parodi R 2000 *Colloids Surf.* A **175** 121
[20] Zhang J, Chi Q, Nielsen J U, Friis E P, Andersen J E T and Ulstrup J 2000 *Langmuir* **16** 7229
[21] Xu Q-M, Wan L-J, Wang C, Bai C-L, Wang Z-Y and Nozawa T 2001 *Langmuir* **17** 6203
[22] Nazmutdinov R R, Zhang J, Zinkicheva T T, Manyurov I R and Ulstrup J 2006 *Langmuir* **22** 7556
[23] Kühnle A, Molina L M, Linderoth T R, Hammer B and Besenbacher F 2004 *Phys. Rev. Lett.* **93** 086101
[24] Cossaro A, Terreni S, Cavalleri O, Prato M, Cvetko D, Morgante A, Floreano L and Canepa M 2006 *Langmuir* **22** 11193
[25] Kühnle A, Linderoth T R, Schunack M and Besenbacher F 2006 *Langmuir* **22** 2156
[26] De Renzi V, Lavagnino L, Corradini V, Biagi R, Canepa M and del Pennino U 2008 *J. Phys. Chem.* C **112** 14439
[27] Cavalleri O, Gonella G, Terreni S, Vignolo M, Floreano L, Morgante A, Canepa M and Rolandi R 2004 *Phys. Chem. Chem. Phys.* **6** 4042
[28] Gonella G, Terreni S, Cvetko D, Cossaro A, Mattera L, Cavalleri O, Rolandi R, Morgante A, Floreano L and Canepa M 2005 *J. Phys. Chem.* B **109** 18003
[29] Beerbom M M, Gargagliano R and Schlaf R 2005 *Langmuir* **21** 3551
[30] Di Felice R, Selloni A and Molinari E 2003 *J. Phys. Chem.* B **107** 1151
[31] Woratschek B, Sesselman W, Küppers J, Ertl G and Haberland H 1987 *Surf. Sci.* **180** 187
[32] Harada Y, Masuda S and Ozaki H 1997 *Chem. Rev.* **97** 1897

[33] Canepa M, Cantini P, Mattera L, Terreni S and Valdenazzi F 1992 *Phys. Scr.* T **41** 226
[34] Canepa M, Mattera L, Polese M and Terreni S 1991 *Chem. Phys. Lett.* **177** 123
[35] Pasquali L, Plesanovas A, Ruocco A, Tarabini A C, Nannarone S, Abbati I, Canepa M, Mattera L and Terreni S 1995 *J. Electron Spectrosc. Relat. Phenom.* **72** 59
[36] Shibata T, Hirooka T and Kuchitsu K 1975 *Chem. Phys. Lett.* **30** 241
[37] Ozaki H and Harada Y 1987 *J. Am. Chem. Soc.* **109** 949
[38] Heinz B and Morgner H 1997 *Surf. Sci.* **372** 100
[39] Suzuki T, Kurahashi M, Ju X and Yamauchi Y 2003 *Appl. Phys. Lett.* **83** 4343
[40] Terzi F, Seeber R, Pigani L, Zanardi C, Pasquali L, Nannarone S, Fabrizio M and Daolio S 2005 *J. Chem. Phys.* B **109** 19397
[41] Pasquali L, Terzi F, Seeber R, Doyle B P and Nannarone S 2008 *J. Chem. Phys.* **128** 134711
[42] Yamauchi Y, Suzuki T, Kurahashi K and Ju X 2003 *J. Phys. Chem.* B **107** 4107
[43] Canepa M, Pelori P, Lavagnino L, Bisio F, Moroni R, Terreni S and Mattera L 2007 *Nucl. Instrum. Methods* B **256** 324
[44] Chenakin S P, Heinz B and Morgner H 1999 *Surf. Sci.* **421** 337
[45] Bonini N, Brivio G P and Trioni M I 2003 *Phys. Rev.* B **68** 035408
[46] Pasquali L, Sapet M C, Staicu-Casagrande M E, Cortona P, Esaulov V A, Nannarone S, Canepa M, Terreni S and Mattera L 2003 *Nucl. Instrum. Methods* B **212** 274
[47] Shin T, Kim K-N, Lee C-W, Shin S K and Kang H 2003 *J. Phys. Chem.* B **107** 11674
[48] Castner D G, Hinds K and Grainger D W 1996 *Langmuir* **12** 5083
[49] Duwez A 2004 *J. Electron Spectrosc. Relat. Phenom.* **134** 97
[50] Di Felice R and Selloni A 2004 *J. Chem. Phys.* **120** 4906
[51] Hermann K, Pettersson L G M, Casida M E, Daul C, Goursot A, Koester A, Proynov E, St-Amant A, Salahub D R, Contributing authors: Carravetta V E, Duarte H, Friedrich C, Godbout N, Guan J, Jamorski C, Leboeuf M, Leetmaa M, Nyberg M, Patchkovskii S, Pedocchi L, Sim F, Triguero L and Vela A 2007 *StoBe-deMon version 3.0*
[52] Hammer B, Hansen L B and Nørskov J K 1999 *Phys. Rev.* B **59** 7413
[53] Perdew J P, Burke K and Ernzerhof M 1996 *Phys. Rev. Lett.* **77** 3865
[54] Godbout N, Salahub D R, Andzelm J and Wimmer E 1992 *Can. J. Chem.* **70** 560
[55] Prato M, Moroni R, Bisio F, Rolandi R, Mattera L, Cavalleri O and Canepa M 2008 *J. Phys. Chem.* C **112** 3899